Advanced Composite Materials
Publication details, including instructions for authors and subscription information:
http://www.tandfonline.com/loi/tacm20

Optimum stacking sequences for extension-twist coupled composites subject to thermal stresses

Serkan Ozbay & Erian A. Armanios

Version of record first published: 02 Apr 2012.

To cite this article: Serkan Ozbay & Erian A. Armanios (2006): Optimum stacking sequences for extension-twist coupled composites subject to thermal stresses, Advanced Composite Materials, 15:2, 127-137

To link to this article: http://dx.doi.org/10.1163/156855106777873932

Adv. Composite Mater., Vol. 15, No. 2, pp. 127–137 (2006)

Also available online - www.vsppub.com

Optimum stacking sequences for extension–twist coupled composites subject to thermal stresses *

SERKAN OZBAY † and ERIAN A. ARMANIOS

School of Aerospace Engineering, Georgia Institute of Technology, Atlanta, GA 30332-0150, USA

Received 14 October 2004; accepted 6 May 2005

Abstract—Optimum stacking sequences for extension–twist coupled composites under thermal stresses are determined. An optimization technique is utilized to determine the optimum stacking sequences. An alternative method is developed based on the identification of a parameter controlling the optimum stacking sequence. Comparison of associated extension–twist coupling values demonstrates their accuracy. It is observed that as the number of plies increases, the optimum stacking sequence follows an asymptotic behavior and that an angle ply system does not represent an optimum stacking sequence. The results are validated through manufacturing of candidate laminates.

Keywords: Extension–twist coupling; thermal stresses; optimum stacking sequences.

1. INTRODUCTION

Elastic tailoring is a distinctive tool in the design of composite structures through which an additional flexibility is provided to meet the design requirements. Couplings between the deformation modes such as extension–twist and bending–twist can be tailored to produce favorable responses. Extension–twist coupling can be achieved in laminated composites by using antisysmmetric stacking sequences. These layups also lead to warping due to temperature changes. This property makes laminated composite structures with antisymmetric stacking sequences unique candidates for passive blade pitch control when subjected to change in temperature, which results in an increase in performance in some applications.

The relatively small torsional-to-extensional stiffness ratio of such laminates leads to finite twisting deformation, which falls beyond the small displacement assumption of classical lamination theory. These effects have been accounted for in the geometrically nonlinear shell-type analysis developed in Ref. [1]. The present work

*Edited by the JSCM.

†To whom correspondence should be addressed. E-mail: serkan_ozbay@ae.gatech.edu

aims at determining the stacking sequences that maximize the twisting response of laminated composites due to temperature change based on the formulation of Ref. [1]. The terms affecting thermal warping are isolated and candidate stacking sequences are determined. A comparison with numerical optimization results is presented. Finally, laminated composite strips with optimum stacking sequences are manufactured and test data compared with analytical and numerical results.

2. METHOD

The fundamental mechanism producing extension–twist coupling in laminated composites is a result of the in-plane extension–shear coupling associated with the off-axis plies. A unidirectional laminate with its fibers making an angle α to the loading direction exhibiting extension–shear coupling is illustrated in Fig. 1a. When subjected to axial loading α_n and $-\alpha_n$ groups of plies would shear in opposite directions. This would generate internal shear forces, shown by the dashed arrows in Fig. 1b, in order to satisfy kinematic continuity conditions. This effectively amounts to an internal twisting moment that induces twisting deformation of the laminate. Intuitively this twisting moment can be maximized using antisymmetric stacking sequences.

The twisting deformation of a laminated strip due to hydrothermal stresses is given by Ref. [1].

$$\Delta T \cdot (a_3 - a_4\theta_0) = 2\psi\theta_0 + a_1\theta_0^2 + a_2\theta_0^3, \tag{1}$$

where ΔT represents the temperature change and θ_0 is the twist rate. The constants a_1, a_2, a_3, a_4 and ψ are functions of the stiffness coefficients and the geometric properties of the strip.

The constitutive relationships for the laminated composite strip are expressed as:

$$\begin{Bmatrix} N_{xx} \\ N_{yy} \\ N_{xy} \\ M_{xx} \\ M_{yy} \\ M_{xy} \end{Bmatrix} = \begin{bmatrix} A_{11} & A_{12} & A_{16} & B_{11} & B_{12} & B_{16} \\ A_{12} & A_{22} & A_{26} & B_{12} & B_{22} & B_{26} \\ A_{16} & A_{26} & A_{66} & B_{16} & B_{26} & B_{66} \\ B_{11} & B_{12} & B_{16} & D_{11} & D_{12} & D_{16} \\ B_{12} & B_{22} & B_{26} & D_{12} & D_{22} & D_{26} \\ B_{16} & B_{26} & B_{66} & D_{16} & D_{26} & D_{66} \end{bmatrix} \begin{Bmatrix} \varepsilon^o_{xx} \\ \varepsilon^o_{yy} \\ \gamma^o_{xy} \\ -\kappa^o_{xx} \\ -\kappa^o_{xx} \\ -\kappa^o_{xy} \end{Bmatrix} - \begin{Bmatrix} N_{xx} \\ N_{yy} \\ N_{xy} \\ M_{xx} \\ M_{yy} \\ M_{xy} \end{Bmatrix}^{HT}, \tag{2}$$

$$\begin{Bmatrix} Q_y \\ Q_x \end{Bmatrix} = \begin{bmatrix} A_{44} & A_{45} \\ A_{45} & A_{55} \end{bmatrix} \begin{Bmatrix} \gamma_{yz} \\ \gamma_{xz} \end{Bmatrix}. \tag{3}$$

The strains and curvatures in equations (2) and (3) account for the finite twist. The inplane, $\boldsymbol{A_{ij}}$, coupling, $\boldsymbol{B_{ij}}$, and bending, $\boldsymbol{D_{ij}}$, stiffness coefficients are defined as

$$\left(A_{ij}, \quad B_{ij}, \quad D_{ij}\right) = \int_{-h/2}^{h/2} \overline{Q}_{ij} \left(1, z, z^2\right) \mathrm{d}z, \tag{4}$$

where $\overline{Q}_{ij}$ are the laminate plane stress-reduced stiffness coefficients defined in the global coordinate system [2]. The hydrothermal forces and moments per unit middle

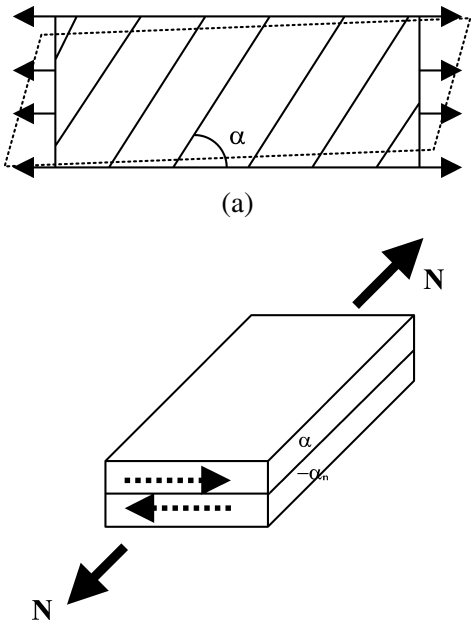

Figure 1. (a) In-plane extension shear coupling; (b) Extension–twist coupling.

surface length denoted by 'HT' in equation (1) are defined as,

$$\left(\left\{ \begin{matrix} N_{xx} \\ N_{yy} \\ N_{xy} \end{matrix} \right\}^{HT} , \left\{ \begin{matrix} M_{xx} \\ M_{yy} \\ M_{xy} \end{matrix} \right\}^{HT} \right)$$

$$= \int_{-h/2}^{h/2} \begin{bmatrix} \overline{Q}_{11} & \overline{Q}_{12} & \overline{Q}_{16} \\ \overline{Q}_{12} & \overline{Q}_{22} & \overline{Q}_{26} \\ \overline{Q}_{16} & \overline{Q}_{26} & \overline{Q}_{66} \end{bmatrix} \begin{bmatrix} \overline{\alpha_{xx}} & \overline{\beta_{xx}} \\ \overline{\alpha_{yy}} & \overline{\beta_{yy}} \\ \overline{\alpha_{xy}} & \overline{\beta_{xy}} \end{bmatrix} \left\{ \begin{matrix} \Delta T \\ \Delta H \end{matrix} \right\} (1, \quad z) \, \mathrm{d}z. \qquad (5)$$

Here α_{ij} and β_{ij}represent the thermal and moisture expansion coefficients, respectively. ΔT refers to the change in temperature while the change in moisture content is denoted by ΔH. For antisymmetric stacking sequences producing extension–twist coupling the following stiffness coefficients vanish

$$A_{16} = A_{26} = B_{11} = B_{22} = B_{12} = B_{66} = D_{16} = D_{26} = 0. \qquad (6)$$

And considering an initially flat laminate subjected to a temperature change only, equation (2) can be rewritten in the following decoupled form.

$$\left\{ \begin{matrix} N_{xx} \\ N_{yy} \\ M_{xy} \end{matrix} \right\}^{HT} = \begin{bmatrix} A_{11} & A_{12} & B_{16} \\ A_{12} & A_{22} & B_{26} \\ B_{16} & B_{26} & D_{66} \end{bmatrix} \left\{ \begin{matrix} \varepsilon_{xx}^{o} \\ \varepsilon_{yy}^{o} \\ -\kappa_{xy} \end{matrix} \right\}, \qquad (7a)$$

$$\begin{Bmatrix} N_{xy} \\ M_{xx} \\ M_{yy} \end{Bmatrix}^{HT} = \begin{bmatrix} A_{66} & B_{16} & B_{26} \\ B_{16} & D_{11} & D_{12} \\ B_{16} & D_{12} & D_{22} \end{bmatrix} \begin{Bmatrix} \gamma_{xy}^{o} \\ \kappa_{xx} \\ -\kappa_{yy} \end{Bmatrix}. \tag{7b}$$

The temperature–twist relationship corresponding to Kirchoff's assumption of no transverse shear strain allows for an accurate prediction of the extension–twist relationship [1], and is given by

$$\Delta T\left(\psi_{12}\bar{\delta}_1 - \psi_{11}\bar{\delta}_2\right) = 2\psi\theta_0 + \frac{b^4\psi_{11}^2}{45}\theta_0^3, \tag{8}$$

where

$$\psi_{11} = A_{11} - \frac{A_{12}^2}{A_{22}}, \quad \psi_{22} = D_{66} - \frac{B_{26}^2}{A_{22}}, \quad \psi_{12} = B_{16} - \frac{A_{12}B_{26}}{A_{22}}, \tag{9a, b, c}$$

$$\bar{\delta}_1 = \frac{1}{\Delta T}\left[N_{xx}^{HT} - \frac{A_{12}}{A_{22}}N_{yy}^{HT}\right], \quad \bar{\delta}_2 = \frac{1}{\Delta T}\left[M_{xy}^{HT} - \frac{B_{26}}{A_{22}}N_{yy}^{HT}\right]. \tag{9d, f}$$

In the present work a further approximation of equation (8) is provided by neglecting the cubic term in the twist-rate.

$$\Delta T\left(\psi_{12}\bar{\delta}_1 - \psi_{11}\bar{\delta}_2\right) = 2\psi\theta_0. \tag{10}$$

Figure 2 shows a comparison of the full solution with the Kirchoff approximation, equation (8), and the proposed approximate solution provided in equation (10) for a thin strip with a stacking sequence of (30/−30). It can be seen that within the

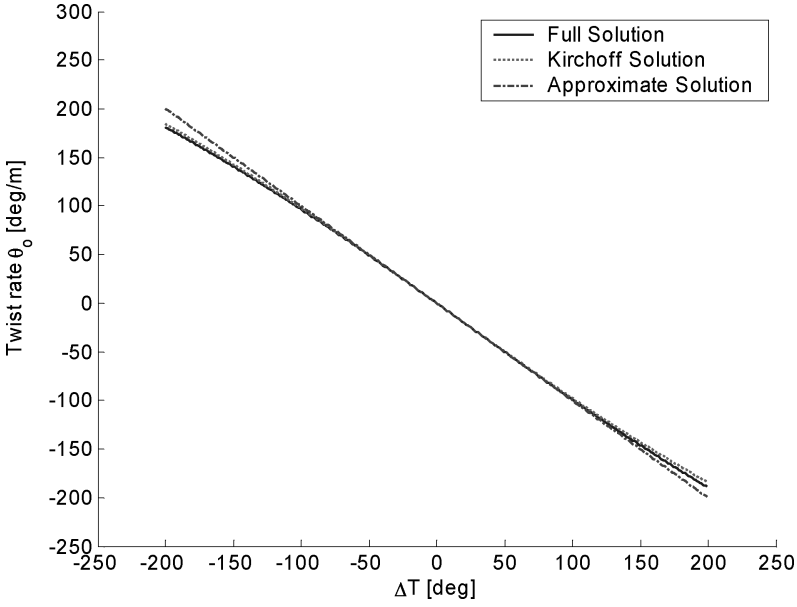

Figure 2. Comparison of full analytical solution with the approximate solutions.

practical range of temperature difference $\Delta T = \pm 150°\text{C}$ the approximate solution shows a close-linear behavior and captures the extension twist behavior with less than 6% maximum error.

The approximate solution given by equation (10) can be rearranged using a set of non-dimensional parameters as follows.

$$1 = \frac{2 \cdot \left(1 - \alpha_1 - \alpha_2 - \alpha_3 + 2\sqrt{\alpha_1\alpha_2\alpha_3}\right)}{\left(\alpha_1 - \sqrt{\alpha_1\alpha_2\alpha_3}\right)\dfrac{N_{xx}^{HT}}{B_{16}} + \left(\alpha_2 - \sqrt{\alpha_1\alpha_2\alpha_3}\right)\dfrac{N_{yy}^{HT}}{B_{26}} - (1 - \alpha_3)\dfrac{M_{xy}^{HT}}{D_{66}}} \cdot \theta_o, \tag{11a}$$

$$\alpha_1 = \frac{B_{16}^2}{A_{11}D_{66}}, \quad \alpha_2 = \frac{B_{26}^2}{A_{22}D_{66}}, \quad \alpha_3 = \frac{A_{12}^2}{A_{11}A_{22}}. \tag{11b, c, d}$$

In this form the main terms determining the extension–twist behavior are represented by the coefficient of the axial hydrothermal load term N_{xx}^{HT} in equation (11a). It is obvious that the extension twist coupling term B_{16} should be increased. However, it should be noted that the N_{xx}^{HT}/B_{16} term is weighted by α_1, which depends on the extension–twist coupling as well as the axial stiffness A_{11} and torsional stiffness D_{66}. This term suggests that an effective extension–twist behavior is achieved not only by increasing the coupling term but also by decreasing the axial and torsional stiffness for the strip.

In a laminated composite the extension–twist coupling stiffness term, B_{16}, is a weighted sum of extension–shear stiffness $\overline{Q}_{16}$ through the thickness of the laminate. An investigation of its variation with ply-angle reveals a maximum value for a 30° ply for the material system considered, as depicted in Fig. 3. This suggests that 30° plies should be selected in order to maximize B_{16}.

The inner plies have less effect on the coupling term B_{16}. In order to maximize α_1 the inner plies should be chosen as close to 90° as possible. In this context, an intuitive $(30/45/90_2/90_2/-45/-30)$ stacking sequence is proposed in order to maximize the extension–twist behavior of a thin strip. In this stacking sequence the outer 30° plies maximize extension–twist coupling stiffness B_{16}. The 45° plies still contribute to maximizing B_{16} while reducing the in-plane axial stiffness A_{11}. Finally, the inner 90° plies play the role of a nonstructural core leading to an increase in the induced shear moment arm while further minimizing the in-plane axial stiffness A_{11} and the torsional stiffness D_{66}.

The variation of thermal load N_{xx}^{HT} with the ply angle is shown in Fig. 4. It should be noted that the 90 degree plies constituting 50% of the intuitive stacking sequence provide high N_{xx}^{HT} values.

3. NUMERICAL OPTIMIZATION

A numerical optimization based on the Sequential Quadratic Programming (SQP) method is utilized to obtain the optimum stacking sequence. A 25.0 mm by 250 mm

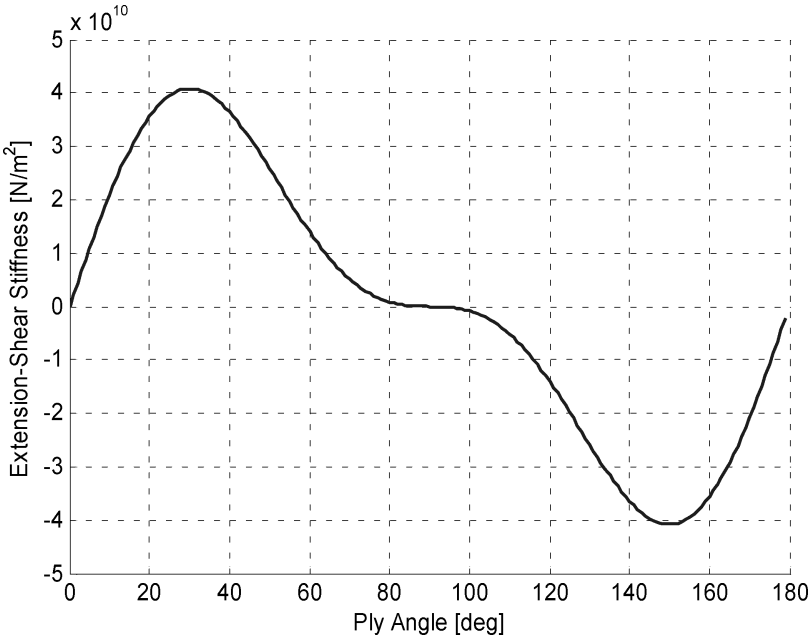

Figure 3. Extension–shear stiffness *vs* ply angle.

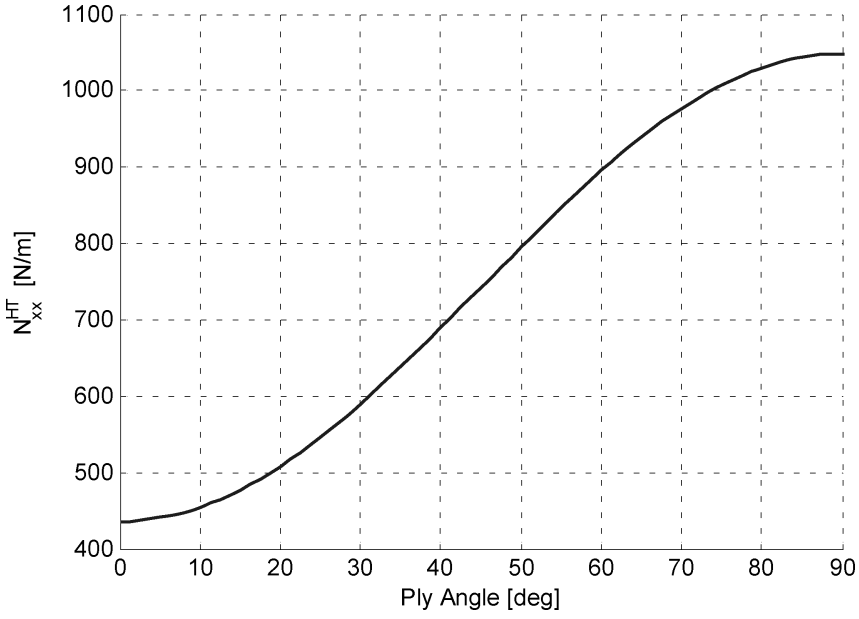

Figure 4. Hydrothermal load N_{xx}^{HT} *vs* ply angle.

laminate with a total constant thickness of 1.248 mm manufactured from IM7/8551-7 Graphite/Epoxy material system is assumed for the optimization. Table 1 provides the material properties for the IM7/8551-7 Graphite/Epoxy material system.

The coefficients of thermal expansion for the system are determined using dilatometry [3]. An Invar-36 bar is used as a reference material and a zero degree laminate as the test material. The strain data is recorded for several temperature cycles between 27° and 65°C for 0 and 90 degree directions and corrected with respect to the apparent strain determined from the reference material. Finally, the coefficient of thermal expansion for the system is determined with a linear best fit to the data. Figure 5 shows a typical corrected strain data, equation (12a), for the specimen.

$$\varepsilon_{\text{corrected}} = \varepsilon_{0,90} - \varepsilon_{\text{ref}}, \tag{12a}$$

$$\alpha_{1,2} = \frac{\varepsilon_{\text{corrected}}}{\Delta T} + \alpha_{\text{ref}}. \tag{12b}$$

Table 1.
Properties of IM7/8551-7 graphite/epoxy material system

Parameters	Values
E_{11}	142.6 GPa
E_{22}	8.39 GPa
G_{12}	3.9 GPa
ν_{12}	0.34
$\bar{\alpha}_1$	0.14 μmm/mm °C
$\bar{\alpha}_2$	30.98 μmm/mm °C
Ply thickness	0.156 mm

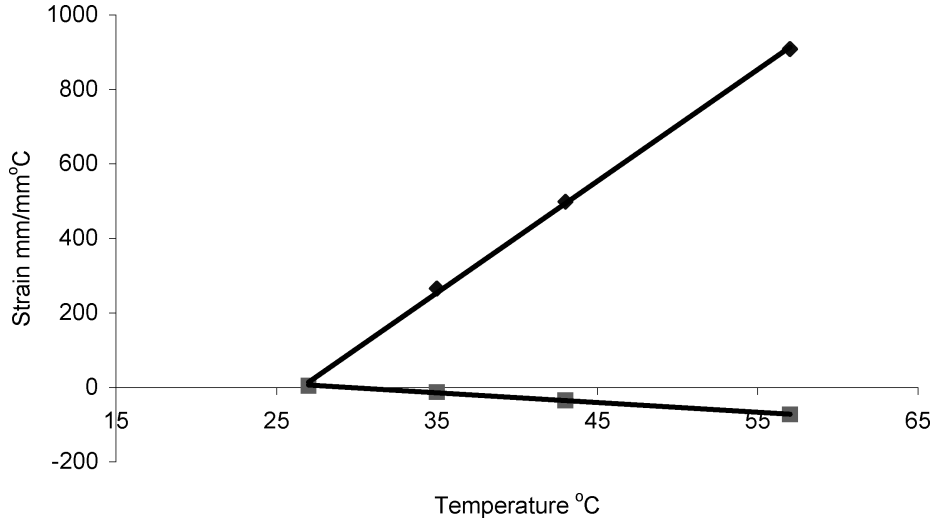

Figure 5. Corrected strain *vs* temperature for IM7/8551-7 graphite/epoxy material system.

The temperature–twist relationship (1) is used for the optimization. For a given constant laminate thickness and varying the number of plies in the stacking sequence, the optimum ply angle distribution is searched for a temperature change of -152°C in order to maximize the twist rate of the laminate. Systems with various numbers of plies, from 2 to 20 plies, are considered in the optimization. As the number of plies increases this in turn causes smaller ply thickness since the laminate thickness is kept constant. The maximum twist obtained versus number of plies with optimum ply angles is provided in Fig. 6. It is observed that the twist rate follows an asymptotic behavior with the increase in number of plies with optimum ply angles. The plot shows more than 30% difference between the laminate with 2-plies and that with 4-plies. This represents the improvement in the maximum twist rate over an angle–ply system. Beyond 4-ply systems the increase in the available twist rate is considerably small within 8% between 4-ply and 12-ply and within 2% between 8-ply and 20-ply systems. For that reason the twist rate corresponding to a highly populated 20-ply system is chosen as the maximum available twist rate for the given material system. Figure 7 illustrates the optimum ply angle distribution through the thickness of a laminate with 20 plies yielding a twist rate of 239.84 degrees/m. The optimum stacking sequence for an 8-ply system is found to be (30.6/41.9/63.9/80.1/$-$80.1/$-$63.9/$-$41.9/$-$30.6) resulting in a twist rate of 234.88 degrees/m.

The validity of the observation made previously regarding the main contribution of the $[B_{16}^2/(A_{11}D_{66})]N_{xx}^{HT}$ parameter to the twist rate is investigated through numerical optimization as well. The stacking sequence which maximizes $[B_{16}^2/(A_{11}D_{66})]N_{xx}^{HT}$ is determined using the SQP based optimization routine.

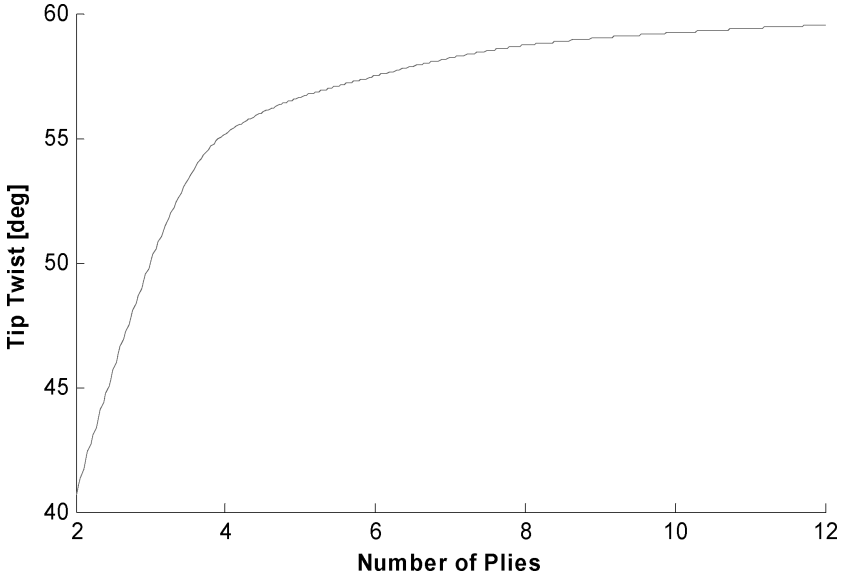

Figure 6. Tip twist *vs* number of plies with optimum stacking sequence.

For an 8-ply laminate the stacking sequence is found to be [31.7/44.9/59.8/76.4/−76.4/−59.8/−44.9/−31.7] leading to 233.32 degrees/m twist rate, which is 2.7% less than the maximum available twist rate of 239.84 degrees/m found earlier. It is also observed for this optimization that, as the number of plies increases, the optimum stacking sequence follows an asymptotic behavior in the tip twist of the laminate as depicted in Fig. 8.

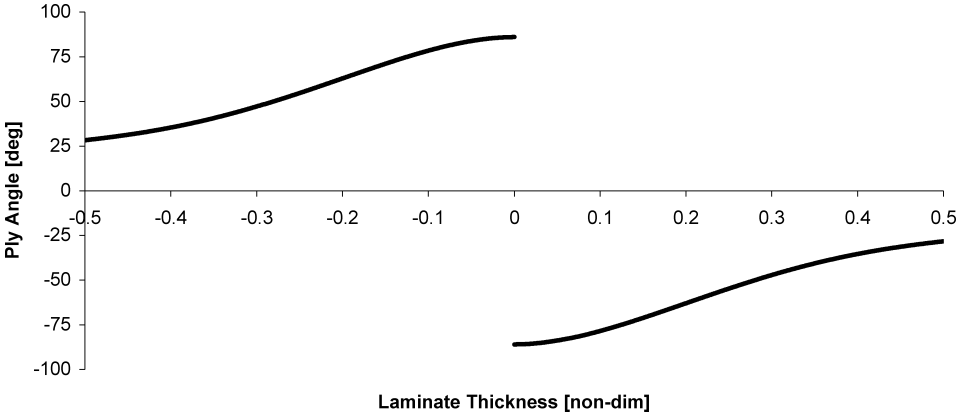

Figure 7. Optimum ply angle distribution through the thickness of the laminate.

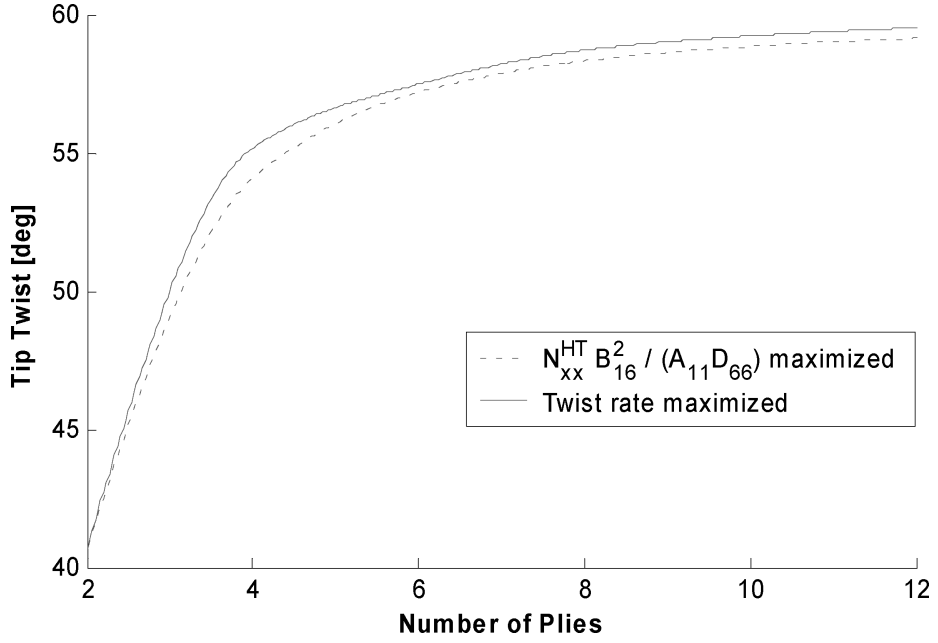

Figure 8. Tip twist *vs* number of plies with optimum stacking sequence.

4. MANUFACTURING AND TESTING

A set of laminates, shown in Table 2, are manufactured to validate the numerical optimization. Manufactured specimens can be seen in Fig. 9. Three specimens for each stacking sequence have been manufactured with the optimum stacking sequence rounded off to the nearest 15° for ease of manufacturing. The angle ply system represents a stacking sequence based on maximizing B_{16}. The comparison of the measured twist rates can be found in Table 3. It is seen that the optimum stacking sequence rounded off to nearest 15° gives on the average 1.5% less twist rate with respect to the numerical optimum solution. The proposed stacking sequence based on maximizing $[B_{16}^2/(A_{11}D_{66})]N_{xx}^{HT}$ provides twist values which are on the average 5.78% lower than the optimum solution. The angle ply system gives twist values that are 38.76% lower on the average.

Table 2.
Manufactured stacking sequences

Stacking sequence	
[30/45/60/75/−75/−60/−45/−30]	Optimum stacking sequence (rounded off to the nearest 15°)
$[30/45/90_2/90_2/-45/-30]$	Proposed stacking sequence based on maximizing $\frac{B_{16}^2}{A_{11}D_{66}}N_{xx}^{HT}$
$[30_4/-30_4]$	Angle ply system (based on maximizing the B_{16})

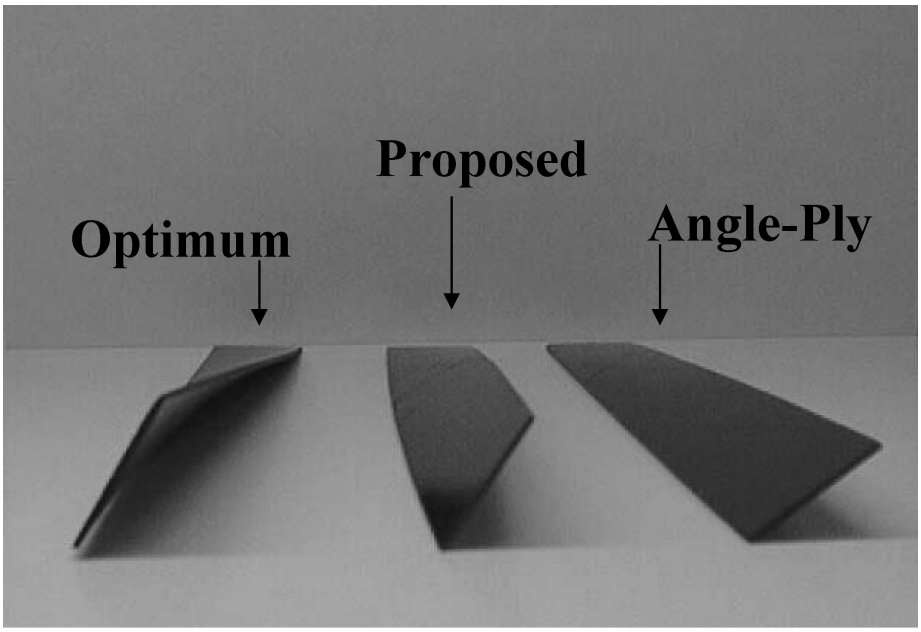

Figure 9. Manufactured specimens.

Table 3.
Comparison of measured twist rates with the numerical optimization result.

Lay-up	Specimen-1 (deg/m)	Specimen-2 (deg/m)	Specimen-3 (deg/m)	Aver. twist rate (deg/m)	% difference w.r.t. num. optimization
[30/45/60/75/−75/−60/−45]	235.1	236.5	237.1	236.2	1.5
$[30/45/90_2/90_2/-45/-30]$	224.7	225.6	227.6	226.0	5.8
$[30_4/-30_4]$	148.9	146.9	144.8	146.9	38.8
Numerical optimization				239.84	

5. CONCLUSION

Optimum stacking sequences for extension–twist coupled composites under thermal stresses are determined. The main term controlling the optimum stacking sequence is identified to be $[B_{16}^2/(A_{11}D_{66})]N_{xx}^{HT}$. Through an optimization routine it is observed that as the number of plies increases, the optimum stacking sequence follows an asymptotic behavior and that angle ply systems do not provide the optimum stacking sequences as they can only be used to maximize the extension–twist coupling term, B_{16}. The optimum and the proposed stacking sequences are manufactured and compared with the numerical solution. The measured twist rates from the proposed stacking sequence confirmed the significance of the controlling parameter resulting in about 6% less twist than the numerical optimum solution.

REFERENCES

1. A. Makeev, E. A. Armanios and D. Hooke, Influence of curing stresses on extension-twist coupling in laminated composite strips, *AIAA Journal* **36**, 1714–1720 (1998).
2. J. R. Vinson and R. L. Sierakowski, *The Behavior of Structures Composed of Composite Materials*. Martinus Nijhoff Publishers, Dordrecht, The Netherlands (1986).
3. Measurement Group, Inc., *Measurement of Thermal Expansion Coefficient Using Strain Gages*, TN-513 (1998).